Fractal-Dependent Growth of Solidlike Condensates

Feipeng Chen,[1] Wei Guo,[1,2] and Ho Cheung Shum[1,2,*]
[1]Department of Mechanical Engineering, The University of Hong Kong, Pokfulam Road, Hong Kong SAR, China
[2]Advanced Biomedical Instrumentation Centre, Hong Kong Science Park, Shatin, New Territories, Hong Kong SAR, China

(Received 13 February 2024; accepted 24 June 2024; published 10 September 2024)

The phenomenon of droplet growth occurs in various industrial and natural processes. Recently, the discovery of liquidlike condensates within cells has sparked an increasing interest in understanding their growth behaviors. These condensates exhibit varying material properties that are closely related to many cellular functions and diseases, particularly during the phase transition from liquidlike droplets to solidlike aggregates. However, how the liquid-to-solid phase transition affects the growth of condensates remains largely unknown. In this study, we investigate the growth of peptide-RNA condensates, which behave as either liquidlike droplets or solidlike aggregates depending on the RNA sequences. Dynamic light scattering experiments show that solidlike condensates grow surprisingly faster, with their hydrodynamic diameters increasing over time as $d_h(t) \sim t^{1/2}$, contrasting with $d_h(t) \sim t^{1/3}$ for liquidlike droplets. By combining theoretical analysis and simulations, we demonstrate that this accelerated growth is caused by the noncoalescence aggregation of solidlike condensates and thus formation of percolated swollen structures with a decreased fractal dimension. Moreover, we demonstrate that the accelerated growth can be slowed down by introducing agents that can revert solidlike condensates back to their liquidlike states, such as urea or specific RNAs. Together, our work reveals a fractal-dependent growth mechanism of condensates, with useful insights for understanding the aging of condensates and modulating their aggregation behaviors in synthetic and biological systems.

DOI: 10.1103/PhysRevLett.133.118401

Droplet growth is a ubiquitous phenomenon observed in a multitude of natural and industrial processes. Classic theories have been widely applied in describing the droplet growth in contexts with different driving forces, such as Brownian motions [1] and Ostwald ripening [2]. Specifically, droplets undergo Brownian motions and coalesce with each other to form larger ones. Alternatively, they can grow without direct contact through Ostwald ripening, where molecules diffuse from smaller droplets to larger ones driven by the difference in Laplace pressure between droplets. Notably, these theories predict that the time evolution of droplet mean radii follows a power law as $r(t) \sim t^{1/3}$. Recent studies have identified similar dropletlike membraneless condensates, formed by the liquid-liquid phase separation of proteins and nucleic acids, within living cells [3]. Prompted by the crucial roles of condensates in cellular functions and diseases, there has been a growing emphasis on comprehending the analogous coarsening behaviors of condensates in living cells [4–6].

Previous studies have introduced several mechanisms to advance our understanding of condensate growth in complex intracellular environments [7–13]. These studies provide important insights into why condensates in cells remain stable over long periods with significantly suppressed coarsening. However, these studies primarily focused on liquidlike condensates, leaving a limited understanding of the growth of solidlike condensates, which often exhibit slow relaxation dynamics and distinct morphologies [14–16]. Importantly, solidlike condensates, formed by liquid-to-solid phase transitions or aging, are closely associated with some neurodegenerative diseases [4,17,18]. Therefore, it is crucial to investigate how the physical properties of condensates impact their growth dynamics.

To address this question, we utilize model condensates consisting of poly-L-lysine and RNAs, resembling biomolecular condensates formed by proteins and nucleic acids [4,16]. In our previous studies, we demonstrated that RNA sequences affect the physical properties of condensates, leading to the formation of either liquidlike droplets or solidlike aggregates [19,20]. These model condensates allow for a quantitative comparison of the growth behaviors of condensates with different physical properties. In this letter, we experimentally observe that solidlike condensates grow more rapidly, with the mean hydrodynamic diameters increasing as $d_h(t) \sim t^{1/2}$, in contrast to liquidlike condensates that grow as $d_h(t) \sim t^{1/3}$. Through theoretical analysis and Monte Carlo simulations, we demonstrate that this rapid growth is caused by the aggregation of solidlike condensates to form swollen fractal structures. Furthermore, we show that the rapid growth of solidlike

*Contact author: ashum@hku.hk.

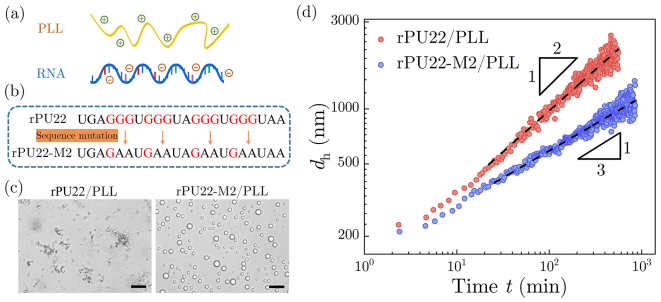

FIG. 1. Coarsening behaviors of condensates with different physical morphologies. (a) Schematic diagram of positively charged PLL and negatively charged single-stranded RNA. (b) Two representative RNAs with (rPU22) and without (rPU22-M2) G-quadruplex (G4) structures. (c) Bright-field images showing different physical morphologies of condensates formed by PLL and rPU22 RNA and rPU22-M2 RNA, respectively, at 1∶1 stoichiometry monomer charge ratio (2 mM PLL, 2 mM RNA, 150 mM KCl, 40 mM Tris buffer, pH = 7.5). The scale bars are 20 μm. (d) Logarithmic plot of hydrodynamic radius (d_h) of condensates over time (10 μM PLL, 10 μM RNA, 150 mM KCl, 40 mM Tris buffer, pH = 7.5). The fitted α (black dashed lines) for rPU22-M2/PLL (blue circles) and rPU22/PLL condensates (red circles) are 0.30 ± 0.004 and 0.45 ± 0.006, respectively.

condensates can be modulated and slowed down by introducing urea and specific RNAs.

We start with condensates formed by poly-L-lysine (PLL) and single-stranded RNAs as model systems. A native 22-nucleotide (nt) single-stranded RNA sequence that contains G-quadruplexes (G4) structures, called rPU22, is used [Fig. 1(a)]. By mutating eight guanine nucleotides into adenine nucleotides, another single-stranded RNA without G4 structures is obtained, named rPU22-M2 [Fig. 1(b)]. Condensates are spontaneously formed by mixing PLL with rPU22 and rPU22-M2 at a 1∶1 stoichiometry charge ratio of lysine to nucleotide, respectively [Fig. 1(c)]. Because of strong interactions between rPU22 and PLL, rPU22/PLL condensates exhibit as solidlike aggregates [Fig. 1(c)]. Their morphologies resemble condensates observed previously in other synthetic systems [16,21–23] and cells [24,25]. In contrast, condensates comprised of rPU22-M2 lacking G4 structures and PLL behave as liquidlike droplets [Fig. 1(c)].

We then characterize the growth behavior of these two condensates using dynamic light scattering (DLS). The results show that the hydrodynamic diameters (d_h) of both types of condensates increase following a power-law relationship over several hours, described as $d_h(t) \sim t^{\alpha}$ with α being the exponent [Fig. 1(d)]. Specifically, the fitted α for rPU22-M2/PLL condensates is about 0.30, while for rPU22/PLL condensates, it is approximately 0.45. This bifurcated trend is consistently observed across experiments conducted at various polymer concentrations (Fig. S1 in the Supplemental Material [26]), collectively showing that α for rPU22-M2/PLL condensates are close to 1/3, while α for rPU22/PLL condensates approach 1/2 (Fig. S1 [26]). In addition, we try another RNA variant, rPU22-M1, which contains 4 guanine-to-adenine nucleotide mutations (Fig. S2a [26]). Bright-field images show the formation of liquidlike condensates upon mixing rPU22-M1 with PLL (Fig. S2b [26]). The fitted α for rPU22-M1/PLL condensates falls within the range of 0.29–0.33 with reasonable experimental variations, consistently approaching 1/3 across different polymer concentrations (Fig. S2c [26]).

To demonstrate the universality of bifurcated coarsening behaviors, we have repeated experiments using other G4-containing RNAs and their mutants. Strong interactions between PLL and RNAs containing G4 structures, such as TERRA and NRAS, result in the formation of solidlike condensates [Figs. 2(a) and 2(b)]. Consistently, these solidlike condensates exhibit rapid coarsening behaviors

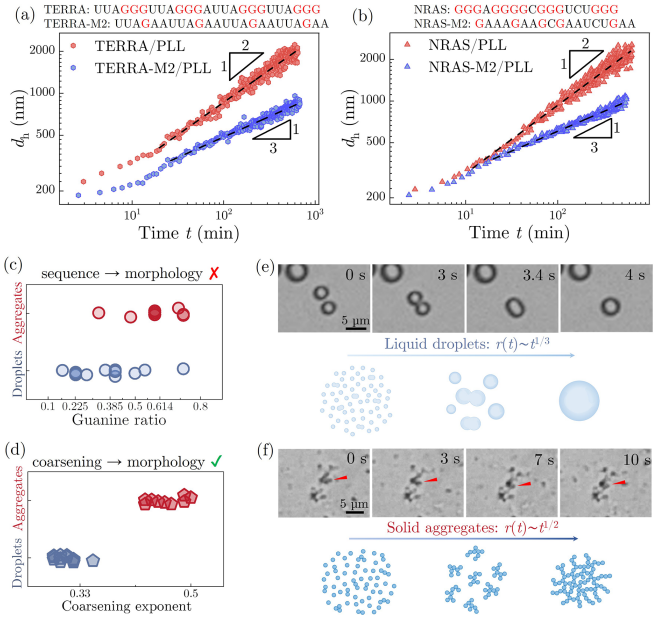

FIG. 2. Universality of bifurcated coarsening behaviors of condensates. (a) Plot of hydrodynamic radius (d_h) over time for TERRA/PLL and TERRA-M2/PLL condensates (10 μM PLL, 10 μM RNA, 150 mM KCl, 40 mM Tris buffer, pH = 7.5). The fitted α are 0.46 ± 0.005 (red circles) and 0.30 ± 0.003 (blue circles), respectively. (b) Plot of hydrodynamic radius (d_h) over time for NRAS/PLL and NRAS-M2/PLL condensates (10 μM PLL, 10 μM RNA, 150 mM KCl, 40 mM Tris buffer, pH = 7.5). The fitted α are 0.49 ± 0.005 (red circles), and 0.29 ± 0.002 (blue circles), respectively. (c) Correlation between physical morphologies of condensates (e.g., aggregates or droplets) and guanine ratio of constituent RNAs. (d) Correlation between physical morphologies and coarsening behaviors of condensates. (e) Bright-filled images and schematic illustration showing that liquid droplets readily merging upon contacting and grow following a power-law function over time as $d_h(t) \sim t^{1/3}$; in contrast, (f) solid aggregates stick together without merging, resulting in a fast coarsening as $d_h(t) \sim t^{1/2}$.

with α close to $1/2$ [Figs. 2(a) and 2(b)]. In contrast, liquidlike droplets formed by PLL and mutated RNAs lacking G4 structures (TERRA-M2 and NRAS-M2) exhibit relatively slower coarsening behaviors with α close to $1/3$ [Figs. 2(a) and 2(b)].

Generally, RNAs enriched in guanine nucleotides have a propensity to form intramolecular and intermolecular G4 secondary structures [30]. To investigate whether the guanine ratio determines the morphologies and coarsening behaviors of condensates, we prepare additional RNA sequences with varying ratios of guanine nucleotides. Interestingly, not all G4-containing RNAs form solidlike aggregates with PLL; for example, TRF, PU22u, and TERRAu RNAs form liquidlike droplets with PLL (Fig. S3 [26]). Moreover, TERRAu-M1 RNA lacking G4 structures can even form solidlike aggregates with PLL (Fig. S4 [26]). Thereby, we do not find a predictive correlation between condensate morphologies and the guanine ratio of constituent RNAs [Fig. 2(c)]. However, regardless of RNA sequences, all solidlike condensates exhibit faster growth with α close to $1/2$, while liquidlike condensates show slower growth with α close to $1/3$ (Fig. S5 [26]). This indicates a strong correlation between the growth behaviors of condensates and their physical morphologies [Fig. 2(d)]. However, what is the underlying mechanism behind this correlation?

To address this question, we look into basic theoretical models of coarsening. The coarsening of liquidlike condensates can be effectively explained by models of Brownian motion-induced coalescence (BMC), which give rise to $d_h(t) \sim t^{1/3}$. In the context of BMC, these liquid droplets grow by merging with each other upon contact, consistent with our experimental observations [Fig. 2(e)]. However, we observe that solidlike condensates grow by sticking to each other rather than merging [Fig. 2(f)], reminiscent of the aggregation behavior seen in colloidal particles [31,32]. Therefore, the non-coalescence of solidlike condensates leads to the formation of percolated structures and may contribute to their fast coarsening behaviors.

In support of this hypothesis, we employ Monte Carlo simulation to investigate the coarsening behaviors of liquid droplets and solid particles. Consistent with experimental findings, liquid droplets can coalesce into larger ones upon contact, whereas solid particles only stick to each other on surfaces in simulations. Importantly, the simulations demonstrate that solid particles grow faster than liquid droplets [Figs. 3(a) and 3(b)]. In particular, the coarsening exponent α for solid particles is approximately $1/2$, which is larger than the $1/3$ observed for liquid droplets [Fig. 3(c)]. These simulation results effectively capture our experimental observations.

However, what theoretical relationship exists between different physical morphologies and the coarsening behaviors of condensates? In statistical mechanics, the growth of a population of droplets or particles undergoing Brownian motions in a homogeneous medium can be described using the Smoluchowski coagulation equation [1,33].

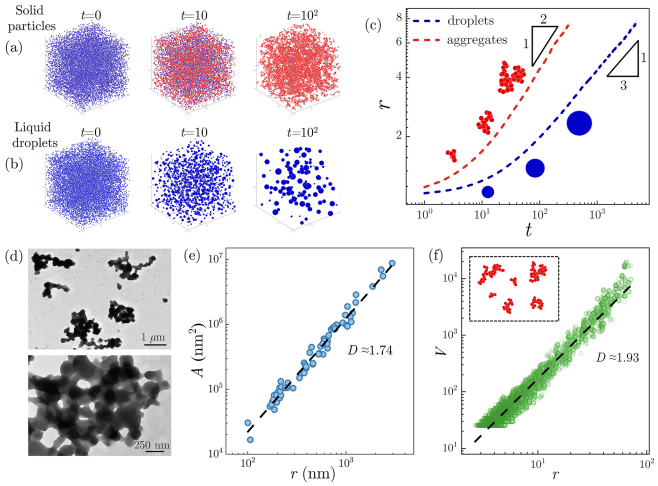

FIG. 3. The decreased fractal dimension of solidlike condensates lead to their fast growth behaviors. (a) (b) Snapshots showing the coarsening of solid particles and liquid droplets at different time points through simulations. Particles that are stuck together in solid aggregates are highlighted as red color in (d). During simulations, a total of 12 000 droplets and particles are placed in three-dimensional $100 \times 100 \times 100$ simulation boxes and allowed to diffuse through Brownian motions and merge or stick upon collision. (c) Plot of mean radius r as a function of time t for liquid droplets (blue) and solid particles (red) in a logarithmic coordinate. Standard deviations (shaded areas) are obtained from 10 simulation replicates with different random seeds. The power-law exponents of coarsening of liquid droplets and solid particles are $1/3$ and $1/2$, respectively, in good agreement with experiments. (d) TEM images showing the fractal morphologies of rPU22/PLL condensates. (e) A logarithmic plot of projected area A as a function of the characteristic radius r of condensates based on TEM images. The fitted fractal dimension is $D = 1.74 \pm 0.03$. (f) Plot of volume V and characteristic radius r of aggregates obtained from Monte Carlo simulations in a logarithmic coordinate. The inset figure shows simulated fractal aggregates that resemble morphologies of solidlike condensates in experiments. The fitted fractal dimension is $D = 1.93 \pm 0.01$.

The detailed derivation and key assumptions of this theory can be found in Supplemental Material, note 1 [26]. The analytical expression of the Smoluchowski coagulation equation is given as

$$\frac{dV}{dt} = \frac{4k_B T \phi_0}{3\eta}, \tag{1}$$

where V is the mean volume of condensates, ϕ_0 is the total volume fraction of condensate phase, η is the viscosity of media, k_B is the Boltzmann constant, and T is the temperature. Following phase separation under fixed conditions, ϕ_0 remains constant as confirmed experimentally and by a theoretical lever rule [34,35]. Therefore, this analytic equation suggests that the mean volume of subjects scales linearly with time as

$$V \sim t. \tag{2}$$

For liquid droplets with $V = (4\pi r^3/3)$, Eq. (1) simplifies to the classic BMC theory: $(dr^3/dt) = (k_B T\phi_0/\pi\eta)$. This theory predicts that the mean size of droplets increases over time as $d_h(t) \sim t^{1/3}$, consistent with the coarsening of liquidlike condensates in our experiments and simulations. In contrast, solidlike condensates exhibit percolated structures, as revealed by transmission electron microscopy (TEM) [Fig. 3(d)]. Notably, a mathematical fractal concept is applied to characterize the volume of these complex structures V as a function of their hydrodynamic radius d_h as $V \sim d_h^D$ where D is the fractal dimension [31,36,37]. For these irregular structures, the fractal dimension is typically noninteger and smaller than the Euclidean dimensionality of space, owing to the presence of neighboring branches and intermediate void spaces. In combination with the coarsening model of $V \sim t$ and the concept of fractal $V \sim d_h^D$, we derive that

$$d_h \sim t^{1/D}. \tag{3}$$

This expression suggests that the coarsening exponent α scales inversely with the fractal dimension D as $\alpha = 1/D$. Based on our previous experiments, it predicts that the fractal dimension of solidlike aggregates should be close to 2. To validate this, we first measure the fractal dimension of solidlike condensates using 2D TEM images. The fractal dimension D is defined as the ratio of the logarithm of the volume V or area A to the logarithm of the characteristic size (see the Supplemental Material for details [26]). The characteristic radius is defined as the radius of the largest circumcircle surrounding a solidlike aggregate throughout the work. By plotting the projected area A as a function of the radius r, we find that the fractal dimension of solidlike condensates is approximately 1.74 [Fig. 3(e)]. This value is close to the fractal dimension of colloidal aggregates at a range of 1.71–1.80, determined using the same methodology in previous studies [38,39]. However, this methodology tends to underestimate the fractal dimension since it approximates the volume of aggregates by their projected area; however, the direct quantification of the volume of aggregates in experiments is challenging due to technical limits. To address this, we use simulations to plot the exact 3D volume V and the characteristic length r of aggregates containing more than 7 unit particles in logarithmic coordinates. From these simulations, the fractal dimension is estimated to be $D \sim 1.93$ [Fig. 3(f)]. This value is slightly higher than that obtained from experiments. In addition, we have demonstrated that the selection of characteristic radius for solidlike condensates does not affect their coarsening exponents. For example, the coarsening exponent of solidlike condensates remains close to $1/2$, regardless of different characteristic radii utilized in simulations (Fig. S8 [26]). The fractal dimensions obtained from both experiments and simulations are close to the theoretically predicted fractal dimension of 2.

In our previous studies, we demonstrated that the solidlike condensates can be melted back to liquidlike counterparts in the presence of urea or G4-free RNAs [Fig. 4(a)] [19]. Therefore, we hypothesize that the growth of solidlike condensates can be regulated by introducing urea or G4-free RNAs [Fig. 4(a)]. To test this, we experimentally monitor the growth of solidlike rPU22/PLL condensates at varying concentrations of urea. Indeed, the coarsening of condensates gradually slows down with increasing urea concentration [Fig. 4(b)]. Particularly, the coarsening exponent transitions from $\sim 1/2$ to $\sim 1/3$ (Fig. S7 [26]). Consequently, we are able to rescale these coarsening data onto a master curve in a plot of $d_h - d_{h0}$ versus t^α, where d_{h0} is the initial hydrodynamic diameter and α is the fitted coarsening exponent (Fig. S9 [26]). In addition, introducing G4-free rPU22-M2 RNA at a 1:1 stoichiometry ratio with rPU22 RNAs also decelerates the growth of solidlike condensates, and the corresponding α returns to approximately $1/3$ (Fig. S6 [26]).

This varying coarsening behavior of condensates is assumed to stem from changes in their fractal dimension. To validate this through simulation, we simplify the model by neglecting the dynamic merging process and assuming that a pair of droplets after merging have equal radii determined by the mass and volume conservation. Additionally, a parameter k, defined as the aspect ratio

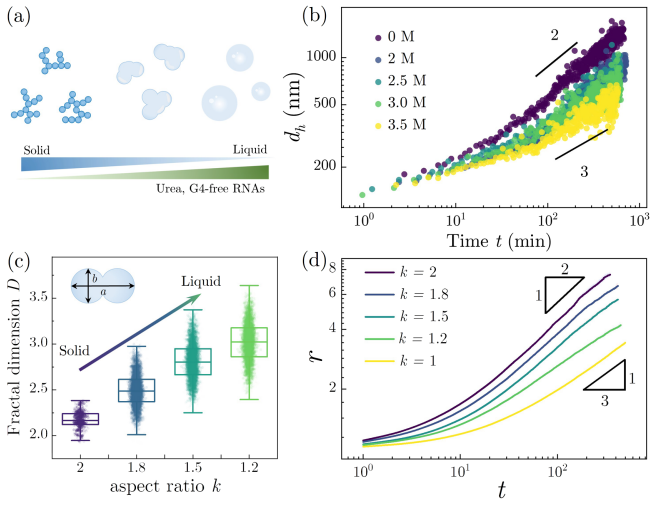

FIG. 4. Tunning growth behaviors of solidlike condensates. (a) Schematic illustrations of the phase transition from solidlike aggregates into liquidlike droplets with increasing concentration of urea and G4-free RNAs. (b) Experimental data showing the slowing growth behaviors of solidlike rPU22/PLL condensates with increasing urea concentration (10 μM PLL, 10 μM RNA, 150 mM KCl, 40 mM Tris buffer, pH = 7.5). (c) The simulations reproduce a decreasing fractal dimension D of clusters with increasing aspect ratio k of neighboring partially merged droplets. (d) Plot of the mean radius of partially merged droplets over time at different aspect ratios k. Curves were obtained by averaging results from ten replicates with different random seeds and the shaded regions below curves indicate the standard deviations (SD).

between the long and short axes of merged droplets [the inset schematic in Fig. 4(c)], is used to describe the merging ratio between a pair of condensate droplets with different physical properties ranging from liquidlike droplets ($k = 1$) to solidlike aggregates ($k = 2$). From the simulations, we observe that the fractal dimension D of aggregates decreases with increasing k [Fig. 4(c)]. Consequently, the growth behavior of condensates gradually slows down, with the coarsening exponent α varying from $1/2$ to $1/3$ [Fig. 4(d)]. These simulation results qualitatively capture the experimental trends shown in Fig. 4(b). Therefore, we demonstrate the ability to tune the growth behaviors of solidlike condensates by adjusting their physical properties through various parameters.

In conclusion, we have introduced a fractal-dependent growth mechanism of condensates. Combining experiments, theory, and simulation, we demonstrate that solidlike condensates exhibit percolated structures with decreased fractal dimensions and fast coarsening behaviors as opposed to their liquidlike counterparts. In particular, it is validated that the coarsening exponent scales inversely with the fractal dimension of condensates as $\alpha = 1/D$. Moreover, we demonstrate the ability to tune the coarsening behaviors of solidlike condensates by introducing urea and G4-free RNAs. Besides our observations, similar percolated solidlike condensates have been observed in various types of synthetic systems [16,21–23] and living cells [24,25]. Therefore, our work provides a generic mechanistic framework for understanding anomalous growth behaviors of solidlike condensates, particularly during liquid-to-solid or aging transitions, in a broad range of synthetic and living systems.

Acknowledgments—The authors thank Xiufeng Li, David A. Weitz, and Yaojun Zhang for their helpful comments on this work. This work is supported by the General Research Fund (No. 17306221, No. 17317322, and No. 17306820) from the Research Grant Council (RGC) of Hong Kong, as well as the National Natural Science Foundation of China (NSFC)-RGC Joint Research Scheme (N_HKU718/19). H. C. S. was funded in part by the Croucher Senior Research Fellowship from Croucher Foundation and the Health@InnoHK program of the Innovation and Technology Commission of the Hong Kong SAR Government.

H. C. Shum is a scientific advisor of EN Technology Limited, MicroDiagnostics Limited, PharmaEase Tech Limited, and Upgrade Biopolymers Limited in which he owns some equity, and also a managing director of the research centre, namely Advanced Biomedical Instrumentation Centre Limited. The works in the paper are however not directly related to the works of these entities. The authors declare no other competing financial interests.

[1] E. D. Siggia, Late stages of spinodal decomposition in binary mixtures, Phys. Rev. A **20**, 595 (1979).
[2] J. H. Yao, K. R. Elder, H. Guo, and M. Grant, Theory and simulation of Ostwald ripening, Phys. Rev. B **47**, 14110 (1993).
[3] C. P. Brangwynne, C. R. Eckmann, D. S. Courson, A. Rybarska, C. Hoege, J. Gharakhani, F. Jülicher, and A. A. Hyman, Germline P granules are liquid droplets that localize by controlled dissolution/condensation, Science **324**, 1729 (2009).
[4] Y. Shin and C. P. Brangwynne, Liquid phase condensation in cell physiology and disease, Science **357** (2017).
[5] S. F. Banani, H. O. Lee, A. A. Hyman, and M. K. Rosen, Biomolecular condensates: Organizers of cellular biochemistry, Nat. Rev. Mol. Cell Biol. **18**, 285 (2017).
[6] J. Berry, C. P. Brangwynne, and M. Haataja, Physical principles of intracellular organization via active and passive phase transitions, Rep. Prog. Phys. **81**, 046601 (2018).
[7] J. Berry *et al.*, RNA transcription modulates phase transition-driven nuclear body assembly, Proc. Natl. Acad. Sci. U.S.A. **112**, E5237 (2015).
[8] D. S. Lee, N. S. Wingreen, and C. P. Brangwynne, Chromatin mechanics dictates subdiffusion and coarsening dynamics of embedded condensates, Nat. Phys. **17**, 531 (2021).
[9] K. A. Rosowski, T. Sai, E. Vidal-Henriquez, D. Zwicker, R. W. Style, and E. R. Dufresne, Elastic ripening and inhibition of liquid-liquid phase separation, Nat. Phys. **16**, 422 (2020).
[10] R. W. Style, T. Sai, N. Fanelli, M. Ijavi, K. Smith-Mannschott, Q. Xu, L. A. Wilen, and E. R. Dufresne, Liquid-liquid phase separation in an elastic network, Phys. Rev. X **8**, 011028 (2018).
[11] Y. Zhang, D. S. W. Lee, Y. Meir, C. P. Brangwynne, and N. S. Wingreen, Mechanical frustration of phase separation in the cell nucleus by chromatin, Phys. Rev. Lett. **126**, 258102 (2021).
[12] K. K. Nakashima *et al.*, Active coacervate droplets are protocells that grow and resist Ostwald ripening, Nat. Commun. **12**, 3819 (2021).
[13] F. Chen, Y. Zhang, and H. C. Shum, Merging-limited coarsening governs long-term stability of nanoscale condensates, bioRxiv, 10.1101/2023.10.06.561146 (2023).
[14] A. Patel *et al.*, A liquid-to-solid phase transition of the ALS protein FUS accelerated by disease mutation, Cell **162**, 1066 (2015).
[15] L. Jawerth *et al.*, Protein condensates as aging Maxwell fluids, Science **370**, 1317 (2020).
[16] Y. Lin, D. S. W. Protter, M. K. Rosen, and R. Parker, Formation and maturation of phase-separated liquid droplets by RNA-binding proteins, Mol. Cell **60**, 208 (2015).
[17] S. Alberti and A. A. Hyman, Biomolecular condensates at the nexus of cellular stress, protein aggregation disease and ageing, Nat. Rev. Mol. Cell Biol. **22**, 196 (2021).
[18] S. Mehta and J. Zhang, Liquid–liquid phase separation drives cellular function and dysfunction in cancer, Nat. Rev. Cancer **22**, 239 (2022).
[19] W. Guo, D. Ji, A. B. Kinghorn, F. Chen, Y. Pan, X. Li, Q. Li, W. T. S. Huck, C. K. Kwok, and H. C. Shum, Tuning material states and functionalities of G-quadruplex-modulated RNA-peptide condensates, J. Am. Chem. Soc. **145**, 2375 (2023).

[20] H. Shum *et al.*, Genetically Encoded DNA-RNA Segregation Stimulates Biomimetic Multiphase Compartments (2024), https://www.researchsquare.com/article/rs-3896193/v1.
[21] J. Van Lindt *et al.*, A generic approach to study the kinetics of liquid-liquid phase separation under near-native conditions, Commun. Biol. **4**, 77 (2021).
[22] H. Strickfaden, T. O. Tolsma, A. Sharma, D. A. Underhill, J. C. Hansen, and M. J. Hendzel, Condensed chromatin behaves like a solid on the mesoscale *in vitro* and in living cells, Cell **183**, 1772 (2020).
[23] G. M. Wadsworth *et al.*, RNAs undergo phase transitions with lower critical solution temperatures, Nat. Chem. 15, 1693 (2023).
[24] Y. Shin, J. Berry, N. Pannucci, M. P. Haataja, J. E. Toettcher, and C. P. Brangwynne, Spatiotemporal control of intracellular phase transitions using light-activated optoDroplets, Cell **168**, 159 (2017).
[25] Y. E. Guo *et al.*, Pol II phosphorylation regulates a switch between transcriptional and splicing condensates, Nature (London) **572**, 543 (2019).
[26] See Supplemental Material at http://link.aps.org/supplemental/10.1103/PhysRevLett.133.118401 for additional information about the experimental methods, simulation methods, notes, and figures, which includes additional Refs. [26–28].
[27] S. F. Shimobayashi, P. Ronceray, D. W. Sanders, M. P. Haataja, and C. P. Brangwynne, Nucleation landscape of biomolecular condensates, Nature (London) **599**, 503 (2021).
[28] M. v. Smoluchowski, Versuch einer mathematischen Theorie der Koagulationskinetik kolloider Lösungen, Z. Phys. Chem. **92**, 129 (1918).
[29] H. Wang and R. H. Davis, Droplet growth due to Brownian, gravitational, or thermocapillary motion and coalescence in dilute dispersions, J. Colloid Interface Sci. **159**, 108 (1993).
[30] K. Lyu, E. Yui-Ching Chow, X. Mou, T.-F. Chan, and C. K. Kwok, RNA G-quadruplexes (rG4s): Genomics and biological functions, Nucleic Acids Res. **49**, 5426 (2021).
[31] D. Weitz, J. S. Huang, M. Y. Lin, and J. Sung, Limits of the fractal dimension for irreversible kinetic aggregation of gold colloids, Phys. Rev. Lett. **54**, 1416 (1985).
[32] M. Lin, H. M. Lindsay, D. A. Weitz, R. C. Ball, R. Klein, and P. Meakin, Universality in colloid aggregation, Nature (London) **339**, 360 (1989).
[33] J. Rogers and R. Davis, Modeling of collision and coalescence of droplets during microgravity processing of Zn-Bi immiscible alloys, Metall. Trans. A **21**, 59 (1990).
[34] S. C. Weber and C. P. Brangwynne, Inverse size scaling of the nucleolus by a concentration-dependent phase transition, Curr. Biol. **25**, 641 (2015).
[35] A. Testa, M. Dindo, A. A. Rebane, B. Nasouri, R. W. Style, R. Golestanian, E. R. Dufresne, and P. Laurino, Sustained enzymatic activity and flow in crowded protein droplets, Nat. Commun. **12**, 6293 (2021).
[36] G. A. Edgar and G. A. Edgar, *Measure, Topology, and Fractal Geometry* (Springer, New York, 2008), Vol. 2.
[37] B. B. Mandelbrot and B. B. Mandelbrot, *The Fractal Geometry of Nature* (W.H. Freeman, New York, 1982), Vol. 1.
[38] P. Meakin, A historical introduction to computer models for fractal aggregates, J. Sol-Gel Sci. Technol. **15**, 97 (1999).
[39] D. Weitz and M. Oliveria, Fractal structures formed by kinetic aggregation of aqueous gold colloids, Phys. Rev. Lett. **52**, 1433 (1984).